



Research article

Analysis of modified Holling-Tanner model with strong Allee effect

Kunlun Huang, Xintian Jia* and Cuiping Li

LMIB-School of Mathematical Sciences, Beihang University, Beijing 100083, China

* **Correspondence:** Email: xintianJ@buaa.edu.cn; Tel:+8618811318750.

Abstract: In this paper, we study a predator-prey system, the modified Holling-Tanner model with strong Allee effect. The existence and stability of the non-negative equilibria are discussed first. Several kinds of bifurcation phenomena, which the model may undergo, such as saddle-node bifurcation, Hopf bifurcation, and Bogdanov-Takens bifurcation, are studied second. Bifurcation diagram for Bogdanov-Takens bifurcation of codimension 2 is given. Then, possible dynamical behaviors of this model are illustrated by numerical simulations. This paper appears to be the first study of the modified Holling-Tanner model that includes the influence of a strong Allee effect.

Keywords: Holling-Tanner model; strong Allee effect; Bogdanov-Takens bifurcation; codimension; coexistence

1. Introduction

Predator-prey is one of three major types of interactions between species besides symbiosis and competition. Understanding the interactions between predators and their prey has been one of the leading research interests in population dynamics [1]. A predator-prey system is dominated by two important factors: the population growth function and the functional response. Tanner [2] presented a predator-prey system in which the environmental carrying capacity of the predator is proportional to the prey population size, and the reduction rate of the prey is proportional to the predator size. It takes the following form:

$$\begin{cases} \frac{dx}{dt} = x \left[r \left(1 - \frac{x}{K} \right) - \frac{ky}{x+D} \right], \\ \frac{dy}{dt} = sy \left(1 - \frac{hy}{x} \right), \end{cases} \quad (1)$$

where $x(t)$ is the prey population and $y(t)$ is the predator population at time t ; r and s are the intrinsic growth rate of the prey and predator respectively; h, k, K and D are all positive parameters. The term

$\frac{kx}{x+D}$ is called Holling-II functional response, generally reflecting the reduction rate of the prey caused by per capita of the predator.

By variable changes:

$$u(\tau) = \frac{x(t)}{K}, \quad v(\tau) = \frac{hy(t)}{K}, \quad \tau = rt, \quad a = \frac{k}{hr}, \quad b = \frac{s}{r}, \quad d = \frac{D}{K},$$

system (1) can be rewritten in a nondimensional form:

$$\begin{cases} \frac{du}{d\tau} = u(1-u) - \frac{auv}{u+d} = f(u, v), \\ \frac{dv}{d\tau} = bv \left(1 - \frac{v}{u}\right) = g(u, v). \end{cases} \quad (2)$$

System (2) has been extensively studied [3–7]. Aziz-Alaoui and Okiye [8] considered the following system with alternative food sources for predators, which is called the modified Holling-Tanner model:

$$\begin{cases} \frac{dx}{dt} = x \left[r \left(1 - \frac{x}{K}\right) - \frac{ky}{x+D} \right], \\ \frac{dy}{dt} = sy \left(1 - \frac{y}{hx + K_2}\right), \end{cases} \quad (3)$$

where $K_2 > 0$, $hx + K_2$ in system (3) is the new carrying capacity for predators. K_2 can be seen as an extra constant carrying capacity from all other food sources for predators. Several researchers [9–15] studied the existence of periodic solutions and bifurcation phenomena of system (3).

Allee effect refers to the phenomenon that low population density inhibits growth. Bioresearch indicates that clustering benefits the growth and survival of species. However, extreme sparsity and overcrowding will prevent population growth and negatively affect reproduction [16–19]. Every species has its optimal density. Species with small population densities are generally vulnerable. Once the population density falls below a critical level, interactions within the species will diminish. Ye et al. [20] considered a predator-prey model with a strong Allee effect and a nonconstant mortality rate. They found that a strong Allee effect may guarantee the coexistence of the species. Hu and Cao [21] considered a predator-prey model with Michaelis-Menten type predator harvesting. Their model exhibits a Bogdanov-Takens bifurcation of codimension 2. Xiang et al. [22] studied the Holling-Tanner model with constant prey harvesting. They found a degenerate Bogdanov-Takens bifurcation of codimension 4 and at least three limit cycles. In [23], Xiang et al. considered the Holling-Tanner model with predator and prey refuge and proved that this model undergoes a Bogdanov-Takens bifurcation of codimension 3. Arancibia et al. [24] adjusted the Holling-Tanner model by adding a strong Allee effect to prey. They found a Bogdanov-Takens bifurcation of codimension 2 and a heteroclinic bifurcation. It seems that a strong Allee effect gives rise to the heteroclinic bifurcation. Jia et al. [25] studied a modified Leslie-Gower model with a weak Allee effect on prey. This model undergoes a degenerate Bogdanov-Takens bifurcation of codimension 3 and has at least two limit cycles. Zhang and Qiao [26] analyzed the SIR model with vaccination and proved that this model undergoes a Bogdanov-Takens bifurcation of codimension 3 in some specific cases.

In this paper, we will analyze the following predator-prey model with the parameter M indicating strong Allee effect:

$$\begin{cases} \frac{dx}{dt} = rx \left(1 - \frac{x}{K}\right) (x - M) - \frac{\alpha xy}{x + m}, \\ \frac{dy}{dt} = sy \left(1 - \frac{\beta y}{x + m}\right), \end{cases} \quad (4)$$

where $\alpha > 0$ and $\beta > 0$ are real numbers. We shall assume $M \ll K$ from now on. If the original population of the prey is less than M , the prey will have a negative growth rate and become extinct ultimately. In system (4), $m > 0$ measures the extent of protection to which the environment provides to prey (or, to predators). It means that the growth rate of prey and predators are not negative infinity when x reduces to zero.

As a first step in analyzing system (4), we nondimensionalize system (4) by writing

$$\frac{x}{K} \rightarrow x, \quad \frac{\alpha y}{rK^2} \rightarrow y, \quad rKt \rightarrow t,$$

and it becomes

$$\begin{cases} \frac{dx}{dt} = x(1-x)(x-a) - \frac{xy}{x+b}, \\ \frac{dy}{dt} = cy \left(1 - \frac{dy}{x+b}\right), \end{cases} \quad (5)$$

where $a = \frac{M}{K} < 1$, $b = \frac{m}{K}$, $c = \frac{s}{rK}$ and $d = \frac{\beta rK}{\alpha}$.

This paper is organized as follows. Section 2 discusses the stability of the equilibria. Section 3 deals with possible bifurcations that system (5) undergoes, such as Hopf bifurcation and Bogdanov-Takens bifurcation. Section 4 summarizes our conclusions.

2. Equilibria and their stability

2.1. Boundary equilibria and their stability

The equilibria of system (5) satisfy the following equations

$$\begin{cases} x(1-x)(x-a) - \frac{xy}{x+b} = 0, \\ cy \left(1 - \frac{dy}{x+b}\right) = 0. \end{cases}$$

We get four boundary equilibria on the axes: $E_0 = (0, 0)$, $E_1 = (1, 0)$, $E_2 = (a, 0)$ and $E_3 = (0, \frac{b}{d})$. These equilibria are all hyperbolic because corresponding linearized matrices at the equilibria E_i ($i = 0, 1, 2, 3$) are

$$J_{E_0} = \begin{pmatrix} -a & 0 \\ 0 & c \end{pmatrix}, \quad J_{E_1} = \begin{pmatrix} a-1 & -\frac{1}{1+b} \\ 0 & c \end{pmatrix},$$

$$J_{E_2} = \begin{pmatrix} a(1-a) & \frac{-a}{a+b} \\ 0 & c \end{pmatrix}, \quad J_{E_3} = \begin{pmatrix} -a - \frac{1}{d} & 0 \\ \frac{c}{d} & -c \end{pmatrix}.$$

Because we have assumed $0 < a < 1$, we get the stability of the boundary equilibria.

Theorem 2.1. System (5) has four equilibria E_i ($i = 0, 1, 2, 3$) on the boundary. $E_0(0, 0)$ and $E_1(1, 0)$ are both hyperbolic saddles, $E_2(a, 0)$ is a hyperbolic unstable node and $E_3(0, \frac{b}{d})$ is a hyperbolic stable node (see Figure 1(c)).

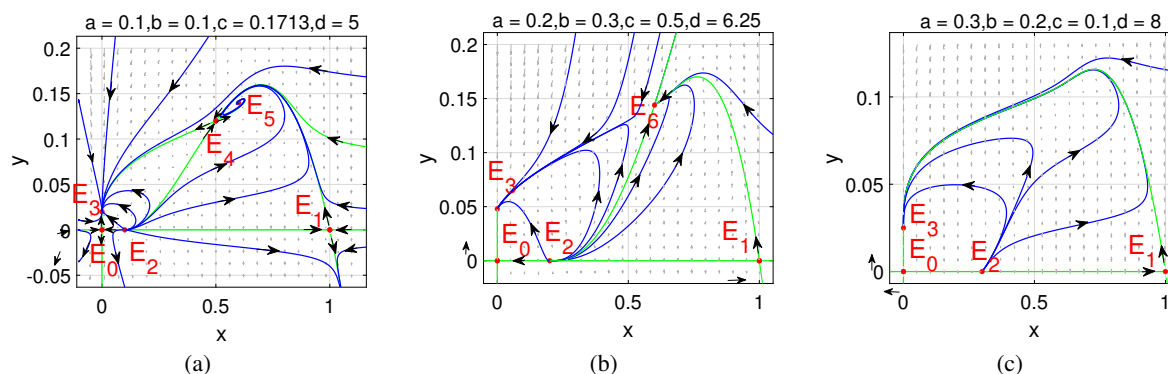


Figure 1. The number of equilibria: (a) 6 equilibria. (b) 5 equilibria. (c) 4 equilibria.

2.2. Positive equilibria and their stability

Theorem 2.2. If $\Delta = (a-1)^2 - \frac{4}{d} > 0$, system (5) has two positive equilibria $E_4(x_4, \frac{x_4+b}{d})$ and $E_5(x_5, \frac{x_5+b}{d})$, where $x_4 = \frac{1+a-\sqrt{\Delta}}{2}$ and $x_5 = \frac{1+a+\sqrt{\Delta}}{2}$. E_4 is always a hyperbolic saddle. E_5 may be a source, a sink or a center depending on the parametric values (see Figure 1(a)).

Proof. The positive equilibria of system (5) satisfy the equations

$$\begin{cases} x^2 - (1+a)x + a + \frac{1}{d} = 0, \\ y = \frac{x+b}{d}. \end{cases}$$

If $\Delta = (a-1)^2 - \frac{4}{d} > 0$, the equation $x^2 - (1+a)x + a + \frac{1}{d} = 0$ has two roots x_i ($i = 4, 5$).

The linearized matrix of system (5) at $E_i = (x_i, \frac{x_i+b}{d})$ ($i = 4, 5$) is

$$J_{E_i} = \begin{pmatrix} -2x_i^2 + (1+a)x_i + \frac{x_i}{d(x_i+b)} & -\frac{x_i}{x_i+b} \\ \frac{c}{d} & -c \end{pmatrix}, \quad i = 4, 5.$$

The determinant of E_4 is $\det J_{E_4} = -cx_4 \sqrt{\Delta} < 0$, from which we get that E_4 is a hyperbolic saddle.

Because $\det J_{E_5} = cx_5 \sqrt{\Delta} > 0$ and $\text{tr} J_{E_5} = -x_5 \sqrt{\Delta} - c + \frac{x_5}{d(x_5+b)}$, the stability of E_5 depends on the parameters a, b, c and d . That is, E_5 is a sink if $\text{tr} J_{E_5} < 0$, a source if $\text{tr} J_{E_5} > 0$.

Theorem 2.3. If $\Delta = (a-1)^2 - \frac{4}{d} = 0$, i.e., $d = \frac{4}{(a-1)^2}$, system (5) has a unique positive equilibrium $E_6(x_6, y_6)$, where $x_6 = \frac{1+a}{2}$ and $y_6 = \frac{1+a+2b}{2d}$ (see Figure 1(b)).

- 1) If $c > \frac{1+a}{d(1+a+2b)}$ ($c < \frac{1+a}{d(1+a+2b)}$), E_6 is an attracting (a repelling) saddle-node;
- 2) If $c = \frac{1+a}{d(1+a+2b)}$, E_6 is a nilpotent cusp of codimension 2 (i.e., the Bogdanov-Takens singularity).

The phase portraits are given in Figure 3.

Proof. The linearized matrix at the equilibrium E_6 is

$$J_{E_6} = \begin{pmatrix} \frac{1+a}{d(1+a+2b)} & -\frac{1+a}{1+a+2b} \\ \frac{c}{d} & -c \end{pmatrix}.$$

E_6 is not hyperbolic because $\det J_{E_6} = 0$. By a shift transformation $x - x_6 \rightarrow x$ and $y - y_6 \rightarrow y$, system (5) becomes

$$\begin{cases} \frac{dx}{dt} = \frac{(1+a)(x-dy)}{d(1+a+2b)} + \left[\frac{4b}{d(1+a+2b)^2} - \frac{1+a}{2} \right] x^2 - \frac{4b}{(1+a+2b)^2} xy + O(|x, y|^3), \\ \frac{dy}{dt} = \frac{c}{d}x - cy - \frac{2c}{d(1+a+2b)}x^2 + \frac{4c}{1+a+2b}xy - \frac{2cd}{1+a+2b}y^2 + O(|x, y|^3). \end{cases} \quad (6)$$

The eigenvalues of J_{E_6} are $\lambda_1 = 0$ and $\lambda_2 = \frac{1+a}{d(1+a+2b)} - c$.

Case 1. $\lambda_2 \neq 0$, i.e., $c \neq \frac{1+a}{d(1+a+2b)}$.

By variable changes

$$\begin{pmatrix} x \\ y \end{pmatrix} = \begin{pmatrix} d & \frac{1+a}{d(1+a+2b)} \\ 1 & \frac{c}{d} \end{pmatrix} \begin{pmatrix} u \\ v \end{pmatrix},$$

system (6) can be rewritten as

$$\begin{cases} \frac{du}{dt} = \frac{cd^2(1+a)}{2\lambda_2}u^2 + O(|u, v|^3), \\ \frac{dv}{dt} = \lambda_2v + O(|u, v|^2). \end{cases} \quad (7)$$

By Theorem 7.1 in chapter 2 of [27], we obtain that E_6 is a saddle-node. There is a parabolic sector neighborhood in which all trajectories approach to E_6 when $\lambda_2 < 0$, and leave it when $\lambda_2 > 0$.

Case 2. $\lambda_2 = 0$, i.e., $c = \frac{1+a}{d(1+a+2b)}$.

According to [28], the cusp is a kind of nonhyperbolic critical point. The cusp can be illustrated by the following example:

$$\begin{cases} \dot{\xi} = \eta, \\ \dot{\eta} = \xi^2. \end{cases}$$

The phase portrait for this system is shown in Figure 2. The neighborhood of the origin consists of two hyperbolic sectors and two separatrices.

Now consider the case when the linearized matrix (denoted as A) has two zero eigenvalues, i.e., $\det A = 0$, $\text{tr} A = 0$, but $A \neq 0$. In this case it is shown in [28], that the system can be put in the normal form:

$$\begin{cases} \dot{\xi} = \eta, \\ \dot{\eta} = a_k \xi^k [1 + h(\xi)] + b_n \xi^n \eta [1 + g(\xi)] + \eta^2 R(\xi, \eta), \end{cases} \quad (8)$$

where $h(\xi)$, $g(\xi)$ and $R(\xi, \eta)$ are analytic in a neighborhood of the origin, $h(0) = g(0) = 0$, $k \geq 2$, $a_k \neq 0$ and $n \geq 1$. The following lemma is given in [28].

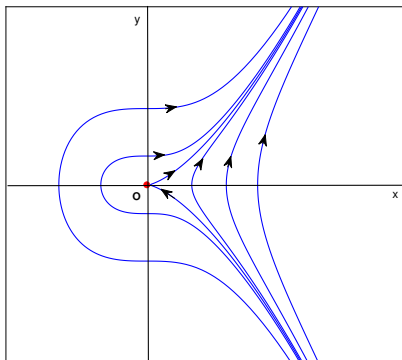


Figure 2. A cusp at the origin.

Lemma 2.1. Let $k = 2m$ with $m \geq 1$ in system (8). Then the type of the origin is given by Table 1.

Table 1. The relationship of b_n, n, m and the type of the origin.

The relationship of b_n, n and m	Type of the origin
$b_n = 0$	Cusp
$b_n \neq 0$ $n \geq m$	Saddle-node
$b_n \neq 0$ $n < m$	Saddle-node

Next, we transform system (6) into a normal form by coordinate transformations. The corresponding linearized matrix of system (6) at E_6 is

$$J_{E_6} = \begin{pmatrix} c & -cd \\ \frac{c}{d} & -c \end{pmatrix}.$$

By variable changes

$$\begin{pmatrix} x \\ y \end{pmatrix} = \begin{pmatrix} d & \frac{d}{c} \\ 1 & 0 \end{pmatrix} \begin{pmatrix} u \\ v \end{pmatrix},$$

system (6) can be rewritten as

$$\begin{cases} \frac{du}{dt} = v - \frac{2d^2}{1+a}v^2 + O(|u, v|^3) \triangleq P(u, v), \\ \frac{dv}{dt} = -\frac{(1+a)^2}{2(1+a+2b)}u^2 - \frac{d[(1+a)^3 + (3+a)(1+3a)b + 4(1+a)b^2]}{(1+a+2b)^2}uv \\ \quad - \frac{d^2(ab+2a+b)}{1+a}v^2 + O(|u, v|^3) \triangleq Q(u, v). \end{cases} \quad (9)$$

Lemma 2.2. ([28]) System (10)

$$\begin{cases} \dot{x} = y + Ax^2 + Bxy + Cy^2 + O(|x, y|^3), \\ \dot{y} = Dx^2 + Exy + Fy^2 + O(|x, y|^3), \end{cases} \quad (10)$$

is equivalent to system (11) near the origin, where system (11) is

$$\begin{cases} \dot{x} = y, \\ \dot{y} = Dx^2 + (E + 2A)xy + O(|x, y|^3). \end{cases} \quad (11)$$

Therefore, by Lemma 2.2, we can transform system (9) into the following form:

$$\begin{cases} \frac{du}{dt} = v, \\ \frac{dv}{dt} = -\frac{(1+a)^2}{2(1+a+2b)}u^2 - \frac{d((1+a)^3 + (3+a)(1+3a)b + 4(1+a)b^2)}{(1+a+2b)^2}uv + O(|u, v|^3). \end{cases} \quad (12)$$

Using the notations of Lemma 2.1, we obtain $k = 2m$, $m = n = 1$, $a_{2m} = -\frac{(1+a)^2}{2(1+a+2b)}$ and $b_n = -\frac{d[(1+a)^3 + (3+a)(1+3a)b + 4(1+a)b^2]}{(1+a+2b)^2}$. Consequently, by Lemma 2.1, we find that $E_6(x_6, y_6)$ is a degenerate critical point (cusp). More exactly, by the results in [28], E_6 is a cusp of codimension 2.

For example, we take $a = 0.1, b = 0.1$ and $d = 4.9383$, which satisfy $(a-1)^2 - \frac{4}{d} = 0$. E_6 is a cusp for $c = \frac{1+a}{d(1+a+2b)} = 0.1713$. E_6 is a saddle-node with parabolic sector approaching it for $c = 0.3$. E_6 is a saddle-node with parabolic sector repelling it for $c = 0.05$ (see Figure 3).

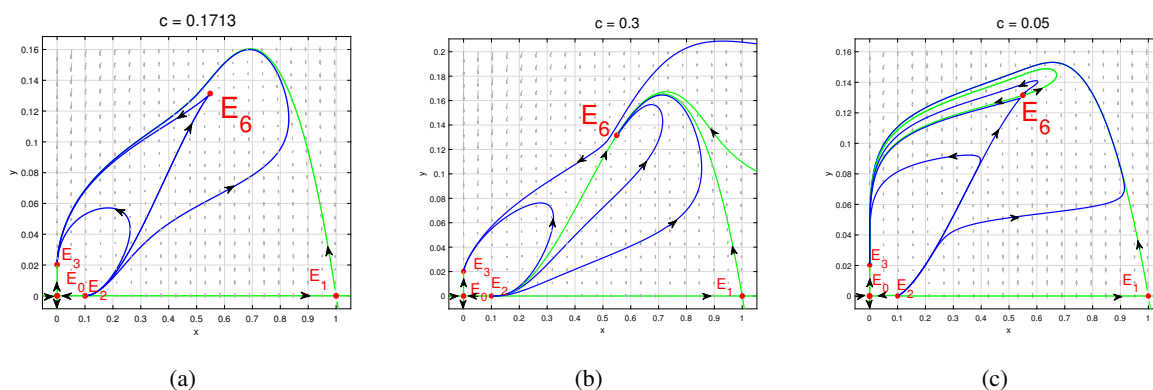


Figure 3. (a) A cusp. (b) A saddle-node ($\lambda_2 < 0$). (c) A saddle-node ($\lambda_2 > 0$).

3. Bifurcation analysis

3.1. Hopf bifurcation

As stated in Theorem 2.2, the positive equilibrium E_5 may be a center, source, or sink because $\det J_{E_5} > 0$. Considering c as the bifurcation parameter, Hopf bifurcation occurs when $c = c_H$, where

c_H satisfies $\text{tr}J_{E_5}|_{c=c_H} = 0$. The local stability of E_5 changes when c passes through $c = c_H$. We summarize our results in the following theorem.

Theorem 3.1. *Hopf bifurcation occurs at E_5 in system (5) when $c = c_H > 0$.*

Proof. Take c as the bifurcation parameter. By $\text{tr}J_{E_5} = -x_5 \sqrt{\Delta} + \frac{x_5}{d(x_5+b)} - c$, we have

$$c_H = -x_5 \sqrt{\Delta} + \frac{x_5}{d(x_5+b)},$$

$$\frac{\partial}{\partial c} \text{tr}J_{E_5}|_{c=c_H} = -1 \neq 0,$$

$$\det J_{E_5} = cx_5 \sqrt{\Delta} > 0.$$

Hopf bifurcation may occur when c crosses c_H .

Next, we discuss the stability of E_5 as $c = c_H$. Moving E_5 to $(0, 0)$ by $X = x + x_5$ and $Y = y + y_5$, the Taylor expansion of system (5) at E_5 takes the form

$$\begin{cases} \frac{dX}{dt} = A_{10}X + A_{01}Y + A_{20}X^2 + A_{11}XY + A_{30}X^3 + A_{21}X^2Y + O(|X, Y|^4), \\ \frac{dY}{dt} = B_{10}X + B_{01}Y + B_{20}X^2 + B_{11}XY + B_{02}Y^2 + B_{30}X^3 + B_{21}X^2Y + B_{12}XY^2 + O(|X, Y|^4), \end{cases} \quad (13)$$

where

$$\begin{aligned} A_{10} &= c_H, \quad A_{01} = -\frac{x_5}{x_5+b}, \quad A_{20} = 1+a-3x_5 + \frac{by_5}{(x_5+b)^3}, \\ A_{11} &= -\frac{b}{(x_5+b)^2}, \quad A_{30} = -1 - \frac{by_5}{(x_5+b)^4}, \quad A_{21} = \frac{b}{(x_5+b)^3}, \\ B_{10} &= \frac{c_H}{d}, \quad B_{01} = -c_H, \quad B_{20} = -\frac{c_H y_5^2 d}{(b+x_5)^3}, \quad B_{11} = \frac{2c_H y_5 d}{(b+x_5)^2}, \\ B_{02} &= -\frac{c_H d}{b+x_5}, \quad B_{30} = \frac{c_H y_5^2 d}{(b+x_5)^4}, \quad B_{21} = -\frac{2c_H y_5 d}{(b+x_5)^3}, \quad B_{12} = \frac{c_H d}{(b+x_5)^2}. \end{aligned}$$

With $\omega = \sqrt{-A_{10}^2 - A_{01}B_{10}} > 0$ and

$$\begin{pmatrix} X \\ Y \end{pmatrix} = \begin{pmatrix} \omega & A_{10} \\ 0 & B_{10} \end{pmatrix} \begin{pmatrix} U \\ V \end{pmatrix}, \text{ i.e., } \begin{pmatrix} U \\ V \end{pmatrix} = \begin{pmatrix} \frac{1}{\omega} & -\frac{d}{\omega} \\ 0 & \frac{1}{B_{10}} \end{pmatrix} \begin{pmatrix} X \\ Y \end{pmatrix},$$

we transform system (13) into the following system

$$\begin{cases} \frac{dU}{dt} = -\omega V + F(U, V), \\ \frac{dV}{dt} = \omega U + G(U, V), \end{cases} \quad (14)$$

where $F(U, V)$ and $G(U, V)$ are the sum of those terms with orders not less than 2.

The stability of $O(0, 0)$ relies on the number

$$\mathcal{K} = \frac{1}{16} (F_{UUU} + F_{UVV} + G_{UUU} + G_{VVV}) \\ + \frac{1}{16\omega} (F_{UV}F_{UU} + F_{UV}F_{VV} + F_{VV}G_{VV}) - \frac{1}{16\omega} (G_{UV}G_{VV} + G_{UV}G_{UU} + F_{UU}G_{UU}).$$

The following simplified expression of \mathcal{K} can be obtained by Maple:

$$\frac{8\mathcal{K}}{c_H} = c_H \left[\frac{2A_{20}^2}{x_5 \sqrt{\Delta}} + \frac{2A_{20}}{x_5 + b} - \left(\frac{2b}{d(x_5 + b)^3} + 3 \right) \right] + \left[2A_{20}^2 + \frac{2x_5 \sqrt{\Delta} A_{20}}{x_5 + b} - 3x_5 \sqrt{\Delta} \left(1 + \frac{b}{d(x_5 + b)^3} \right) \right] \\ + \left[\frac{c_H b^2}{(x_5 + b)^4 d^2 x_5 \sqrt{\Delta}} - \frac{A_{20} b}{d(x_5 + b)^2} - \frac{3c_H A_{20} b}{x_5 \sqrt{\Delta} d(x_5 + b)^2} \right] = I_1 + I_2 + I_3,$$

$$\Delta = (a - 1)^2 - \frac{4}{d} < (1 - a)^2, \quad x_5 = \frac{1 + a + \sqrt{\Delta}}{2} > \sqrt{\Delta}, \quad c_H = \frac{x_5}{d(x_5 + b)} - x_5 \sqrt{\Delta} > 0,$$

$$A_{20} = 1 + a - 3x_5 - \frac{b}{d(x_5 + b)^2} < -(x_5 + \sqrt{\Delta}) - \frac{b}{d(x_5 + b)^2} < 0,$$

$$\frac{I_1}{c_H} = \frac{2A_{20}^2}{x_5 \sqrt{\Delta}} + \frac{2A_{20}}{x_5 + b} - \left(\frac{2b}{d(x_5 + b)^3} + 3 \right) \\ = \frac{A_{20}}{x_5 \sqrt{\Delta}} \left(A_{20} + \frac{2x_5 \sqrt{\Delta}}{x_5 + b} \right) + \frac{1}{x_5 \sqrt{\Delta}} \left(A_{20}^2 - 3x_5 \sqrt{\Delta} - \frac{2bx_5 \sqrt{\Delta}}{d(x_5 + b)^3} \right) \\ > \frac{A_{20}}{x_5 \sqrt{\Delta}} \left(-(x_5 + \sqrt{\Delta}) + 2\sqrt{\Delta} \right) + \frac{1}{x_5 \sqrt{\Delta}} \left((x_5 + \sqrt{\Delta})^2 - 3x_5 \sqrt{\Delta} \right) + \frac{2b \left(x_5 + \sqrt{\Delta} - \frac{x_5 \sqrt{\Delta}}{x_5 + b} \right)}{d(x_5 + b)^2 x_5 \sqrt{\Delta}} > 0,$$

$$I_2 = 2A_{20}^2 + \frac{2x_5 \sqrt{\Delta} A_{20}}{x_5 + b} - 3x_5 \sqrt{\Delta} \left(1 + \frac{b}{d(x_5 + b)^3} \right) \\ = A_{20} \left(A_{20} + \frac{2x_5 \sqrt{\Delta}}{x_5 + b} \right) + \left(A_{20}^2 - 3x_5 \sqrt{\Delta} \left(1 + \frac{b}{d(x_5 + b)^3} \right) \right) \\ > A_{20} \left(-(x_5 + \sqrt{\Delta}) + 2\sqrt{\Delta} \right) + \left((x_5 + \sqrt{\Delta})^2 - 3x_5 \sqrt{\Delta} \right) + \frac{b}{d(x_5 + b)^2} \left(2(x_5 + \sqrt{\Delta}) - \frac{3x_5 \sqrt{\Delta}}{x_5 + b} \right) > 0,$$

$$I_3 = \frac{c_H b^2}{(x_5 + b)^4 d^2 x_5 \sqrt{\Delta}} - \frac{A_{20} b}{d(x_5 + b)^2} - \frac{3c_H A_{20} b}{x_5 \sqrt{\Delta} d(x_5 + b)^2}.$$

It is obvious that $I_3 > 0$ because all the elements are positive. Therefore, E_5 undergoes a subcritical bifurcation when $c = c_H$. When $c > c_H$ and $|c - c_H| \ll \varepsilon$, there is an unstable limit cycle (see Figure 4(b)).

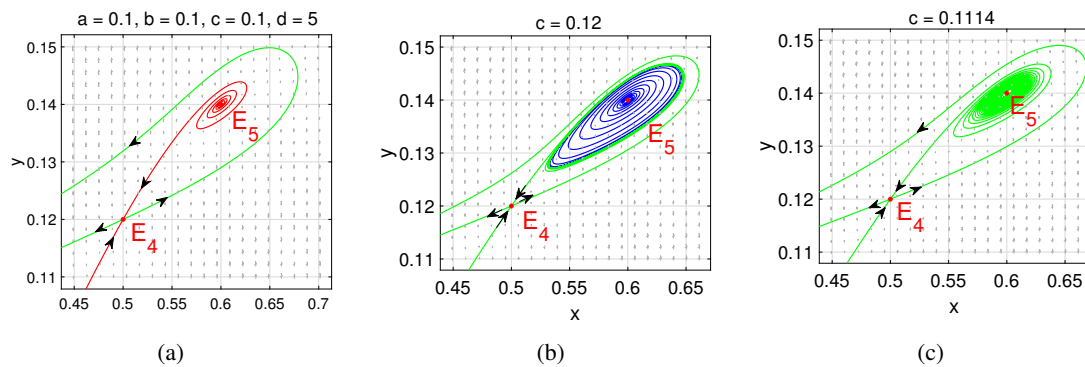


Figure 4. Hopf Bifurcation of system (5): (a) E_5 is an unstable focus. (b) E_5 is a stable focus and there is an unstable closed orbit. (c) E_5 is a linear center.

3.2. Bogdanov-Takens bifurcation

Theorem 3.2. When c and d are selected as two bifurcation parameters, $\det J_{E_5}|_{(c,d)=(c_{BT},d_{BT})} = 0$ and $\text{tr} J_{E_5}|_{(c,d)=(c_{BT},d_{BT})} = 0$, system (5) undergoes a Bogdanov-Takens bifurcation of codimension 2 in a small neighborhood of E_5 as (c, d) varies near $(c_{BT}, d_{BT}) = (\frac{(a-1)^2}{4} \frac{1+a}{1+a+2b}, \frac{4}{(a-1)^2})$.

Proof. Perturb parameters c and d by $c = c_{BT} + \varepsilon_1$ and $d = d_{BT} + \varepsilon_2$, where $(\varepsilon_1, \varepsilon_2)$ is sufficiently small, and system (5) takes the following form:

$$\begin{cases} \frac{dx}{dt} = x(1-x)(x-a) - \frac{xy}{x+b}, \\ \frac{dy}{dt} = (c_{BT} + \varepsilon_1)y \left(1 - \frac{(d_{BT} + \varepsilon_2)y}{x+b}\right). \end{cases} \tag{15}$$

The Taylor expansion of system (15) at $E_5(x_5, y_5)$ is

$$\begin{cases} \frac{dx}{dt} = p_{10}x + p_{01}y + p_{20}x^2 + p_{11}xy + O(|x, y, \varepsilon_1, \varepsilon_2|^3), \\ \frac{dy}{dt} = q_{00} + q_{10}x + q_{01}y + q_{11}xy + q_{02}y^2 + O(|x, y, \varepsilon_1, \varepsilon_2|^3), \end{cases} \tag{16}$$

where

$$\begin{aligned} p_{10} &= -2x_5^2 + (1+a)x_5 + \frac{x_5}{d(x_5+b)}, & p_{01} &= -\frac{x_5}{x_5+b}, & p_{20} &= 1+a-3x_5 + \frac{by_5}{(x_5+b)^3}, \\ p_{11} &= -\frac{b}{(x_5+b)^2}, & q_{00} &= -\frac{\varepsilon_2 y_5 (c_{BT} + \varepsilon_1)}{d_{BT}}, & q_{10} &= \frac{(c_{BT} + \varepsilon_1)(d_{BT} + \varepsilon_2)}{d_{BT}^2}, \\ q_{01} &= (c_{BT} + \varepsilon_1) \left(1 - \frac{2(d_{BT} + \varepsilon_2)}{d_{BT}}\right), & q_{11} &= \frac{2(c_{BT} + \varepsilon_1)(d_{BT} + \varepsilon_2)}{d_{BT}(x_5+b)}, & q_{02} &= -\frac{(c_{BT} + \varepsilon_1)(d_{BT} + \varepsilon_2)}{x_5+b}. \end{aligned}$$

Take a C^∞ change of coordinates around $(0, 0)$

$$u_1 = x, \quad v_1 = \frac{dx}{dt},$$

then system (16) is changed into the following form

$$\begin{cases} \dot{u}_1 = v_1, \\ \dot{v}_1 = n_{00} + n_{10}u_1 + n_{01}v_1 + n_{20}u_1^2 + n_{11}u_1v_1 + n_{02}v_1^2 + O(|u_1, v_1, \varepsilon_1, \varepsilon_2|^3), \end{cases} \quad (17)$$

where

$$\begin{aligned} n_{00} &= p_{01}q_{00}, \quad n_{10} = p_{01}q_{10} - p_{10}q_{01} + p_{11}q_{00}, \quad n_{01} = p_{10} + q_{01}, \\ n_{20} &= q_{20}p_{01} - q_{11}p_{10} + p_{11}q_{10} - q_{01}p_{20} + \frac{p_{10}^2q_{02}}{p_{01}}, \\ n_{11} &= 2p_{20} + q_{11} - \frac{p_{11}p_{10} + 2q_{02}p_{10}}{p_{01}}, \quad n_{02} = \frac{p_{11} + q_{02}}{p_{01}}. \end{aligned}$$

After rescaling the time by $(1 - n_{02}u_1)t \rightarrow t$, system (17) is rewritten as

$$\begin{cases} \dot{u}_1 = v_1(1 - n_{02}u_1), \\ \dot{v}_1 = (1 - n_{02}u_1) \left[n_{00} + n_{10}u_1 + n_{01}v_1 + n_{20}u_1^2 + n_{11}u_1v_1 + n_{02}v_1^2 + O(|u_1, v_1, \varepsilon_1, \varepsilon_2|^3) \right]. \end{cases} \quad (18)$$

Letting $u_2 = u_1$ and $v_2 = v_1(1 - n_{02}u_1)$, we get system (19) as follows

$$\begin{cases} \dot{u}_2 = v_2, \\ \dot{v}_2 = \theta_{00} + \theta_{10}u_2 + \theta_{01}v_2 + \theta_{20}u_2^2 + \theta_{11}u_2v_2 + O(|u_2, v_2, \varepsilon_1, \varepsilon_2|^3), \end{cases} \quad (19)$$

where

$$\begin{aligned} \theta_{00} &= n_{00}, \quad \theta_{10} = n_{10} - 2n_{00}n_{02}, \quad \theta_{01} = n_{01}, \\ \theta_{20} &= n_{20} - 2n_{10}n_{02} + n_{00}n_{02}^2, \quad \theta_{11} = n_{11} - n_{01}n_{02}. \end{aligned}$$

Case 1: For small ε_i ($i = 1, 2$), if $\theta_{20} > 0$, by the following change of variables

$$u_3 = u_2, \quad v_3 = \frac{v_2}{\sqrt{\theta_{20}}}, \quad t \rightarrow \sqrt{\theta_{20}}t,$$

system (19) becomes

$$\begin{cases} \dot{u}_3 = v_3, \\ \dot{v}_3 = s_{00} + s_{10}u_3 + s_{01}v_3 + u_3^2 + s_{11}u_3v_3 + O(|u_3, v_3, \varepsilon_1, \varepsilon_2|^3), \end{cases} \quad (20)$$

where

$$s_{00} = \frac{\theta_{00}}{\theta_{20}}, \quad s_{10} = \frac{\theta_{10}}{\theta_{20}}, \quad s_{01} = \frac{\theta_{01}}{\sqrt{\theta_{20}}}, \quad s_{11} = \frac{\theta_{11}}{\sqrt{\theta_{20}}}.$$

To eliminate the u_3 term, letting $u_4 = u_3 + \frac{s_{10}}{2}$ and $v_4 = v_3$, we get system (21) as follows

$$\begin{cases} \dot{u}_4 = v_4, \\ \dot{v}_4 = r_{00} + r_{01}v_4 + u_4^2 + r_{11}u_4v_4 + O(|u_4, v_4, \varepsilon_1, \varepsilon_2|^3), \end{cases} \quad (21)$$

where

$$r_{00} = s_{00} - \frac{s_{10}^2}{4}, \quad r_{01} = s_{01} - \frac{s_{10}s_{11}}{2}, \quad r_{11} = s_{11}.$$

Clearly, $r_{11} = s_{11} = \frac{\theta_{11}}{\sqrt{\theta_{20}}} \neq 0$ if $\theta_{11} \neq 0$.

Setting $u_5 = r_{11}^2 u_4$, $v_5 = r_{11}^3 v_4$ and $\tau = \frac{1}{r_{11}} t$, we obtain the universal unfolding of system (16)

$$\begin{cases} \dot{u}_5 = v_5, \\ \dot{v}_5 = \mu_1 + \mu_2 v_5 + u_5^2 + u_5 v_5 + O(|u_5, v_5, \varepsilon_1, \varepsilon_2|^3), \end{cases} \quad (22)$$

where

$$\mu_1 = r_{00} r_{11}^4, \quad \mu_2 = r_{01} r_{11}. \quad (23)$$

Case 2: For small $\varepsilon_i (i = 1, 2)$, if $\theta_{20} < 0$, by the following change of variables

$$u'_3 = u_2, \quad v'_3 = \frac{v_2}{\sqrt{-\theta_{20}}}, \quad t \rightarrow \sqrt{-\theta_{20}} t,$$

system (19) becomes

$$\begin{cases} \dot{u}'_3 = v'_3, \\ \dot{v}'_3 = s'_{00} + s'_{10} u_3 + s'_{01} v_3 - u_3^2 + s'_{11} u_3 v_3 + O(|u_3, v_3, \varepsilon_1, \varepsilon_2|^3), \end{cases} \quad (24)$$

where

$$s'_{00} = -\frac{\theta_{00}}{\theta_{20}}, \quad s'_{10} = -\frac{\theta_{10}}{\theta_{20}}, \quad s'_{01} = \frac{\theta_{01}}{\sqrt{-\theta_{20}}}, \quad s'_{11} = \frac{\theta_{11}}{\sqrt{-\theta_{20}}}.$$

To eliminate the u_3 term, letting $u'_4 = u'_3 - \frac{s'_{10}}{2}$ and $v'_4 = v'_3$, we get system (25) as follows

$$\begin{cases} \dot{u}'_4 = v'_4, \\ \dot{v}'_4 = r'_{00} + r'_{01} v'_4 - u_4^2 + r'_{11} u'_4 v'_4 + O(|u'_4, v'_4, \varepsilon_1, \varepsilon_2|^3), \end{cases} \quad (25)$$

where

$$r'_{00} = s'_{00} + \frac{s_{10}^2}{4}, \quad r'_{01} = s'_{01} + \frac{s'_{10}s'_{11}}{2}, \quad r'_{11} = s'_{11}.$$

Clearly, $r'_{11} = s'_{11} = \frac{\theta_{11}}{\sqrt{-\theta_{20}}} \neq 0$ if $\theta_{11} \neq 0$.

Setting $u'_5 = -r_{11}^2 u'_4$, $v'_5 = r_{11}^3 v'_4$ and $\tau = -\frac{1}{r_{11}} t$, we obtain the universal unfolding of system (16)

$$\begin{cases} \dot{u}'_5 = v'_5, \\ \dot{v}'_5 = \mu'_1 + \mu'_2 v'_5 + u_5^2 + u_5 v_5 + O(|u'_5, v'_5, \varepsilon_1, \varepsilon_2|^3), \end{cases} \quad (26)$$

where

$$\mu'_1 = -r'_{00} r_{11}^4, \quad \mu'_2 = -r'_{01} r_{11}. \quad (27)$$

Retain μ_1 and μ_2 to denote μ'_1 and μ'_2 . If the matrix $\left. \frac{\partial(\mu_1, \mu_2)}{\partial(\varepsilon_1, \varepsilon_2)} \right|_{\varepsilon_1=\varepsilon_2=0}$ is nonsingular, the parameter transformations (23) and (27) are homeomorphisms in a small neighborhood of $(0, 0)$, and μ_1, μ_2 are independent parameters. Direct computation shows that $\theta_{20} = -\frac{(1+a)^2(a-1)^2(a^2+2ab+2b^2+2b+1)}{4(1+a+2b)^3} < 0$ when $\varepsilon_i = 0$ ($i = 1, 2$) and

$$\left. \frac{\partial(\mu_1, \mu_2)}{\partial(\varepsilon_1, \varepsilon_2)} \right|_{\varepsilon_1=\varepsilon_2=0} = -\frac{2(a^3 + (3b+3)a^2 + (4b^2 + 10b + 3)a + 4b^2 + 3b + 1)^5 (1+a+2b)}{(a^2 + 2ab + 2b^2 + 2b + 1)^4 (1+a)^6 (a-1)^2} \neq 0.$$

By Perko [28], we know that systems (22) and (26) undergo the Bogdanov-Takens bifurcation when $\varepsilon = (\varepsilon_1, \varepsilon_2)$ is in a small neighborhood of the origin. The local representations of the unfolding bifurcation curves are as follows (“+” for $\theta_{20} > 0$, “-” for $\theta_{20} < 0$):

- 1) The saddle-node bifurcation curve $\text{SN} = \{(\varepsilon_1, \varepsilon_2) : \mu_1(\varepsilon_1, \varepsilon_2) = 0, \mu_2(\varepsilon_1, \varepsilon_2) \neq 0\}$;
- 2) The Hopf bifurcation curve $\text{H} = \{(\varepsilon_1, \varepsilon_2) : \mu_2(\varepsilon_1, \varepsilon_2) = \pm \sqrt{-\mu_1(\varepsilon_1, \varepsilon_2)}, \mu_1(\varepsilon_1, \varepsilon_2) < 0\}$;
- 3) The homoclinic bifurcation curve $\text{HOM} = \{(\varepsilon_1, \varepsilon_2) : \mu_2(\varepsilon_1, \varepsilon_2) = \pm \frac{5}{7} \sqrt{-\mu_1(\varepsilon_1, \varepsilon_2)}, \mu_1(\varepsilon_1, \varepsilon_2) < 0\}$.

For example, in system (15), we can set $a = 0.1$, $b = 0.1$ and $d_{BT} = \frac{4}{(a-1)^2} \approx 4.93827$. Further computation yields $x_5 = \frac{1+a}{2} = 0.55$, $y_5 = \frac{x_5+b}{d} = 0.131625$ and $c_{BT} = -2x_5^2 + (1+a)x_5 + \frac{x_5}{d(x_5+b)} \approx 0.171346$. Since

$$\left. \frac{\partial(\mu_1, \mu_2)}{\partial(\varepsilon_1, \varepsilon_2)} \right|_{\varepsilon_1=\varepsilon_2=0} = \begin{vmatrix} 0 & -1.74742 \\ -7.54666 & -0.323622 \end{vmatrix} \approx -13.1872 \neq 0,$$

the parametric transformation (27) is nonsingular. Moreover, $\theta_{20} = -0.139409 - 0.81361\varepsilon_1 - 0.058426\varepsilon_2 - 0.340982\varepsilon_1\varepsilon_2 < 0$ and $\theta_{11} = -1.05207 + 1.81818\varepsilon_1 + 0.126173\varepsilon_2 + 8.97868\varepsilon_1^2 + 1.67098\varepsilon_1\varepsilon_2 + 0.021619\varepsilon_2^2 \neq 0$ for small ε_i ($i = 1, 2$). The local representations of the bifurcation curves of system (15) up to second-order approximations are as follows. The details of the computation are given in Appendix.

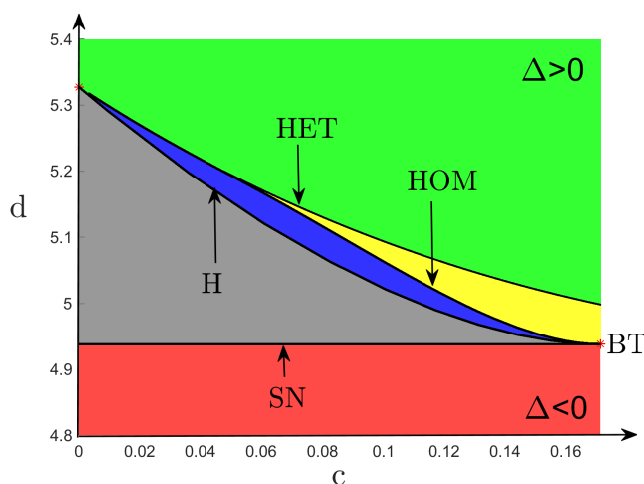


Figure 5. Bifurcation diagram of the parameter c and d with $a = 0.1$ and $b = 0.1$.

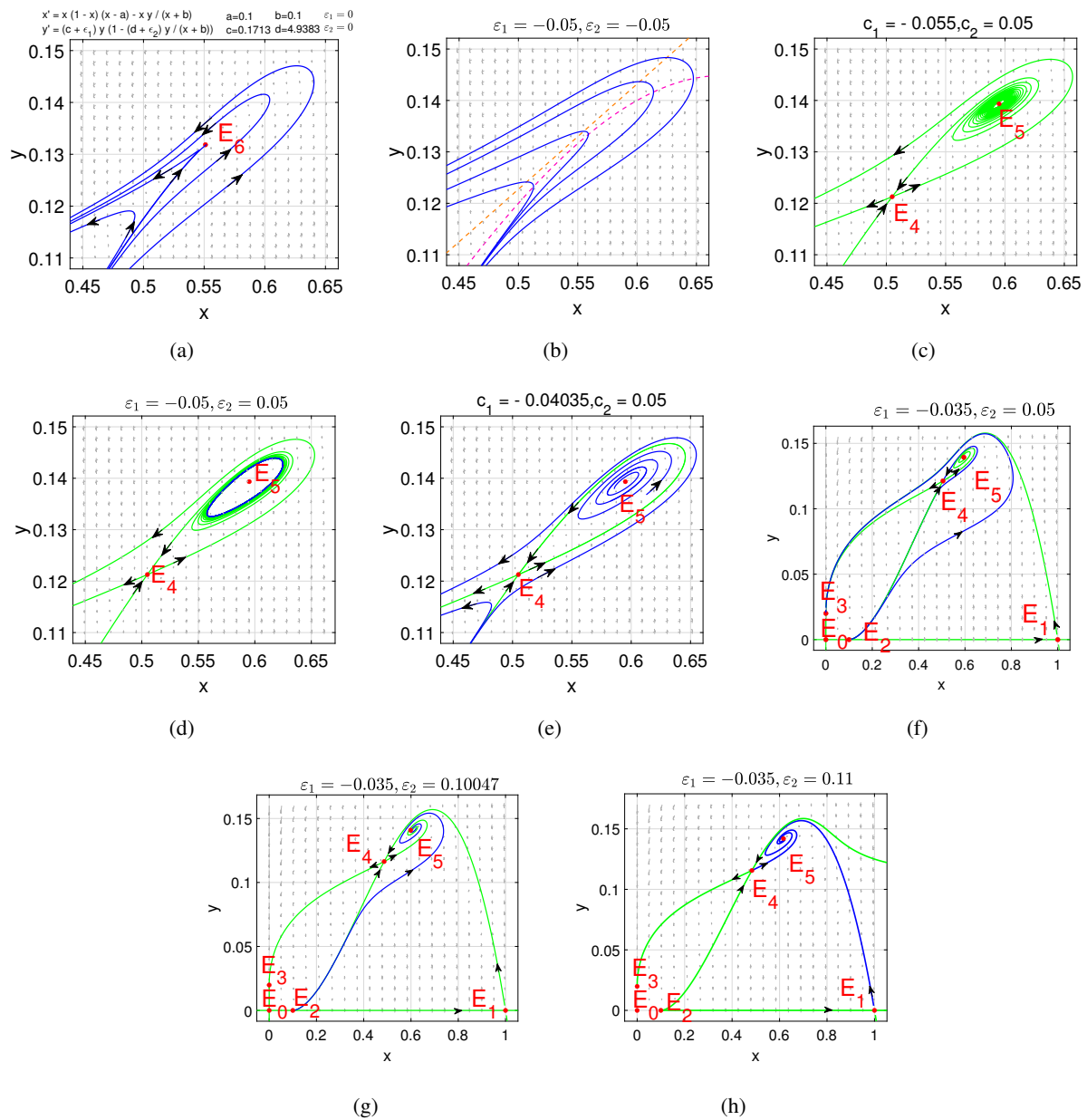


Figure 6. Phase portraits of system (5): (a) A cusp point. (b) There is no positive equilibrium. (c) A saddle and an unstable focus. (d) An unstable limit cycle and a stable focus. (e) An unstable homoclinic cycle. (f) A saddle and a stable focus. (g) E_1 connects with E_4 . (h) E_1 connects with E_5 .

- 1) The saddle-node bifurcation curve SN, is expressed as $\{(\varepsilon_1, \varepsilon_2) : \varepsilon_2 = 0, \varepsilon_1 < 0\}$;
- 2) The Hopf bifurcation curve H, is expressed as

$$\{(\varepsilon_1, \varepsilon_2) : -1.74742\varepsilon_2 + 56.9521\varepsilon_1^2 + 37.3603\varepsilon_1\varepsilon_2 + 3.09997\varepsilon_2^2 = 0, \varepsilon_1 < 0\};$$

- 3) The homoclinic bifurcation curve HOM, is expressed as

$$\{(\varepsilon_1, \varepsilon_2) : -1.74742\varepsilon_2 + 111.626\varepsilon_1^2 + 42.0495\varepsilon_1\varepsilon_2 + 3.20051\varepsilon_2^2 = 0, \varepsilon_1 < 0\};$$

4) The heteroclinic bifurcation curve HET, can be detected with MATCONT, the numerical bifurcation package.

- (a) When $(\varepsilon_1, \varepsilon_2) = (0, 0)$, E_5 is a cusp of codimension 2 (see Figure 6(a)).
- (b) When $(\varepsilon_1, \varepsilon_2)$ is below SN, there are no positive equilibria (see Figure 6(b)).
- (c) When $(\varepsilon_1, \varepsilon_2)$ crosses the SN curve and locates in the area between H and SN, there are two positive equilibria E_4 and E_5 . E_4 is a saddle and E_5 is unstable (see Figure 6(c)).
- (d) When $(\varepsilon_1, \varepsilon_2)$ crosses H, an unstable limit cycle will appear (see Figure 6(d)).
- (e) When $(\varepsilon_1, \varepsilon_2)$ is on the curve HOM, there is an unstable homoclinic orbit (see Figure 6(e)).
- (f) When $(\varepsilon_1, \varepsilon_2)$ is between the curve HOM and HET, E_4 connects with E_2 (see Figure 6(f)).
- (g) When $(\varepsilon_1, \varepsilon_2)$ falls on the HET curve, E_4 connects with E_1 (see Figure 6(g)).
- (h) When $(\varepsilon_1, \varepsilon_2)$ crosses the HET curve, E_1 connects with E_5 (see Figure 6(h)).

4. Conclusions

This paper considers the modified Holling-Tanner model with a strong Allee effect. The aim is to explore the dynamical behaviors occurring in the predator-prey model with a strong Allee effect and alternative food sources for predators. Section 2 considers the equilibria and their stability. There exist four equilibria on the boundary. $E_0(0, 0)$ and $E_1(1, 0)$ are saddles, $E_2(a, 0)$ is an unstable node and $E_3(0, \frac{b}{d})$ is a stable node. As for the positive equilibria, when $d < \frac{4}{(a-1)^2}$, there is no positive equilibrium. When $d = \frac{4}{(a-1)^2}$, saddle-node bifurcation occurs and there is a unique positive equilibrium E_6 , which is a cusp when $c = \frac{(a-1)^2}{4} \frac{1+a}{1+a+2b}$ and a saddle-node when $c \neq \frac{(a-1)^2}{4} \frac{1+a}{1+a+2b}$. When $d > \frac{4}{(a-1)^2}$, the saddle-node E_6 separates into two positive equilibria, a saddle E_4 and a hyperbolic equilibrium E_5 . We examine the local stability of E_5 and find that E_5 is stable if $c > c_H$ and unstable if $c < c_H$. In Section 3.1, we prove that system (5) undergoes a Hopf bifurcation near E_5 when $c = c_H$ by showing that the constant $\mathcal{K} > 0$. In Section 3.2, we prove that system (5) exhibits a Bogdanov-Takens bifurcation of codimension 2 by calculating the universal unfolding near the cusp E_6 . Besides, we give the bifurcation diagram with a little perturbation $(\varepsilon_1, \varepsilon_2)$ added to (c_{BT}, d_{BT}) .

Our main result is that, after adding a strong Allee effect and alternative food sources, system (5) allows the independent survival of predators. In addition, a strong Allee effect makes the system more stable. Since, in the original Holling-Tanner system (2), there are at least two limit cycles [29], while after adding a strong Allee effect, there seems to be a unique stable limit cycle [24].

From the ecological viewpoint, alternative food sources for predators help them survive without prey. Besides, a strong Allee effect makes prey extinct at low density. Codimension of the Bogdanov-Takens bifurcation is at most two and the Hopf bifurcation is nondegenerate. We compare Holling-Tanner models with and without a strong Allee effect. It is found that a strong Allee effect increases and changes the dynamics. The first is that a strong Allee effect introduces saddle-node bifurcation. Second, heteroclinic bifurcation is brought about by the Allee effect, which means that the prey and predators may take different paths to reach distinct ultimate states. These indicate that the ecosystem may be sensitive to disturbances. It is essential to be aware of such bifurcations and protect the environment to weaken the Allee effect. In the future, we plan to study the system with different environmental protection for prey and predators. We will introduce m_1 and m_2 in place of b to system (5) and consider

the following equation:

$$\begin{cases} \dot{x} = rx \left(1 - \frac{x}{K}\right) (x - M) - \frac{\alpha xy}{x+m_1}, \\ \dot{y} = sy \left(1 - \frac{\beta y}{x+m_2}\right). \end{cases} \quad (28)$$

If the functional response depends on the time as well as the prey and predator population, the model could exhibit more interesting dynamical behavior even chaos. We will do some research in our future works.

Use of AI tools declaration

The authors declare they have not used Artificial Intelligence (AI) tools in the creation of this article.

Acknowledgments

This work was supported by National Natural Science Foundation of China (Grant No.62227810).

Conflict of interest

The authors declare there is no conflict of interest.

References

1. P. H. Leslie, Some further notes on the use of matrices in population mathematics, *Biometrika*, **35** (1948), 213–245. <https://doi.org/10.2307/2332342>
2. J. T. Tanner, The stability and the intrinsic growth rates of prey and predator populations, *Ecology*, **56** (1975), 855–867. <https://doi.org/10.2307/1936296>
3. Y. Kuang, Global stability of Gause-type predator-prey systems, *J. Math. Biol.*, **28** (1990), 463–474. <https://doi.org/10.1007/BF00178329>
4. G. J. Butler, S. B. Hsu, P. Waltman, Coexistence of competing predators in a chemostat, *J. Math. Biol.*, **17** (1983), 133–151. <https://doi.org/10.1007/BF00305755>
5. K. S. Cheng, S. B. Hsu, S. S. Lin, Some results on global stability of a predator-prey system, *J. Math. Biol.*, **12** (1982), 115–126. <https://doi.org/10.1007/BF00275207>
6. S. B. Hsu, T. W. Hwang, Hopf bifurcation analysis for a predator-prey system of Holling and Leslie type, *Taiwan. J. Math.*, **3** (1999), 35–53. <https://doi.org/10.11650/twjtm/1500407053>
7. S. B. Hsu, T. W. Huang, Global stability for a class of predator-prey systems, *SIAM. J. Appl. Math.*, **55** (1995), 763–783. <https://doi.org/10.1137/S0036139993253201>
8. M. A. Aziz-Alaoui, M. D. Okiye, Boundedness and global stability for a predator-prey model with modified Leslie-Gower and Holling-type II schemes, *Appl. Math. Lett.*, **16** (2013), 1069–1075. [https://doi.org/10.1016/S0893-9659\(03\)90096-6](https://doi.org/10.1016/S0893-9659(03)90096-6)
9. C. Xiang, J. C. Huang, H. Wang, Linking bifurcation analysis of Holling-Tanner model with generalist predator to a changing environment, *Stud. Appl. Math.*, **149** (2022), 124–163. <https://doi.org/10.1111/sapm.12492>

10. Y. H. Du, R. Peng, M. X. Wang, Effect of a protection zone in the diffusive Leslie predator-prey model, *J. Differ. Equations*, **246** (2009), 3932–3956. <https://doi.org/10.1016/j.jde.2008.11.007>
11. R. P. Gupta, P. Chandra, Bifurcation analysis of modified Leslie-Gower predator-prey model with Michaelis-Menten type prey harvesting, *J. Math. Anal. Appl.*, **398** (2013), 278–295. <https://doi.org/10.1016/j.jmaa.2012.08.057>
12. Y. L. Zhu, W. Kai, Existence and global attractivity of positive periodic solutions for a predator-prey model with modified Leslie-Gower Holling-type II schemes, *J. Math. Anal. Appl.*, **384** (2011), 400–408. <https://doi.org/10.1016/j.jmaa.2011.05.081>
13. C. Ji, D. Jiang, N. Shi, Analysis of a predator-prey model with modified Leslie-Gower and Holling-type II schemes with stochastic perturbation, *J. Math. Anal. Appl.*, **359** (2009), 482–498. <https://doi.org/10.1016/j.jmaa.2009.05.039>
14. J. Xie, H. Liu, D. Luo, The Effects of harvesting on the dynamics of a Leslie-Gower model, *Discrete Dyn. Nat. Soc.*, **2** (2021), 1–11. <https://doi.org/10.1155/2021/5520758>
15. Z. Shang, Y. Qiao, Bifurcation analysis of a Leslie-type predator-prey system with simplified Holling type IV functional response and strong Allee effect on prey, *Nonlinear Anal.: Real World Appl.*, **64** (2022), 103–453. <https://doi.org/10.1016/j.nonrwa.2021.103453>
16. Y. Huang, Z. Zhu, Z. Li, Modeling the Allee effect and fear effect in predator-prey system incorporating a prey refuge, *Adv. Differ. Equations*, **321** (2020), 1–13. <https://doi.org/10.1186/s13662-020-02727-5>
17. D. Sen, S. Ghorai, S. Sharma, M. Banerjee, Allee effect in prey's growth reduces the dynamical complexity in prey-predator model with generalist predator, *Appl. Math. Modell.*, **91** (2021), 768–790. <https://doi.org/10.1016/j.apm.2020.09.046>
18. A. Kumar, B. Dubey, Dynamics of prey-predator model with strong and weak Allee effect in the prey with gestation delay, *Nonlinear Anal.-Model. Control*, **25** (2020), 417–442. <https://doi.org/10.15388/namc.2020.25.16663>
19. V. Méndez, C. Sans, I. Lopus, D. Campos, Extinction conditions for isolated populations with Allee effect, *Math. Biosci.*, **232** (2011), 78–86. <https://doi.org/10.1103/PhysRevE.99.022101>
20. J. Ye, Y. Wang, Z. Jin, C. J. Dai, M. Zhao, Dynamics of a predator-prey model with strong allee effect and nonconstant mortality rate, *Math. Biosci. Eng.*, **19** (2022), 3402–3426. <https://doi.org/10.3934/mbe.2022157>
21. D. Hu, H. Cao, Stability and bifurcation analysis in a predator-prey system with Michaelis-Menten type predator harvesting, *Nonlinear Anal.: Real World Appl.*, **33** (2017), 58–82. <https://doi.org/10.1016/j.nonrwa.2016.05.010>
22. C. Xiang, J. C. Huang, M. Lu, Degenerate Bogdanov-Takens bifurcation of codimension 4 in Holling-Tanner model with harvesting, *J. Differ. Equations*, **314** (2022), 370–417. <https://doi.org/10.1016/j.jde.2022.01.016>
23. C. Xiang, J. C. Huang, H. Wang, Bifurcations in Holling-Tanner model with generalist predator and prey refuge, *J. Differ. Equations*, **343** (2023), 495–529. <https://doi.org/10.1016/j.jde.2022.10.018>

24. C. Arancibia-Ibarra, J. D. Flores, G. Pettet, P. V. Heijster, A Holling-Tanner predator-prey model with strong Allee effect, *Int. J. Bifurcation Chaos*, **29** (2019), 1–16. <https://doi.org/10.1142/S0218127419300325>
25. X. T. Jia, K. L. Huang, C. P. Li, Bifurcation analysis of a modified Leslie-Gower predator-prey System, *Int. J. Bifurcat. Chaos*, **33** (2023), 1–16. <https://doi.org/10.1142/S0218127423500244>
26. J. J. Zhang, Y. H. Qiao, Bifurcation analysis of an SIR model considering hospital resources and vaccination, *Math. Comput. Simul.*, **208** (2023), 157–185. <https://doi.org/10.1016/j.matcom.2023.01.023>
27. Z. F. Zhang, T. R. Ding, W. Z. Huang, Z. X. Dong, *Qualitative Theory of Differential Equations*, *Amer. Math. Soc.*, **101** (1992). <https://doi.org/10.1090/mmono/101>
28. L. Perko, *Differential Equations and Dynamical Systems*, 3rd edition, Springer-Verlag, New York, 2013. <https://doi.org/10.1007/978-1-4613-0003-8>
29. A. Gasull, Limit cycles in the Holling-Tanner model, *Publ. Mat.*, **41** (1997), 149–167. http://doi.org/10.5565/PUBLMAT_41197_09

Appendix

For $a = 0.1$, $b = 0.1$, system (16) takes the form

$$\begin{cases} \frac{dx}{dt} = p_{10}x + p_{01}y + p_{20}x^2 + p_{11}xy + O(|x, y, \varepsilon_1, \varepsilon_2|^3), \\ \frac{dy}{dt} = q_{00} + q_{10}x + q_{01}y + q_{11}xy + q_{02}y^2 + O(|x, y, \varepsilon_1, \varepsilon_2|^3), \end{cases} \quad (\text{A.1})$$

where

$$\begin{aligned} p_{10} &= 0.171346, & p_{01} &= -0.846154, & p_{20} &= -0.502071, & p_{11} &= -0.236686, \\ q_{00} &= -0.004567\varepsilon_2, & q_{10} &= 0.034698 + 0.2025\varepsilon_1 + 0.007026\varepsilon_2, \\ q_{01} &= -0.171346 - \varepsilon_1 + 0.069395\varepsilon_2, & q_{11} &= 0.527219 + 3.076923\varepsilon_1 + 0.106762\varepsilon_2, \\ q_{02} &= -1.301775 - 7.597341\varepsilon_1 - 0.263609\varepsilon_2. \end{aligned}$$

Take a C^∞ change of coordinates around $(0, 0)$

$$u_1 = x, \quad v_1 = \frac{dx}{dt},$$

then system (A.1) is changed into the following form

$$\begin{cases} \dot{u}_1 = v_1, \\ \dot{v}_1 = n_{00} + n_{10}u_1 + n_{01}v_1 + n_{20}u_1^2 + n_{11}u_1v_1 + n_{02}v_1^2 + O(|u_1, v_1, \varepsilon_1, \varepsilon_2|^3), \end{cases} \quad (\text{A.2})$$

where

$$\begin{aligned} n_{00} &= 0.003864\varepsilon_2, & n_{10} &= 0.007026\varepsilon_2, & n_{01} &= -\varepsilon_1 - 0.069395\varepsilon_2, \\ n_{20} &= -0.139409 - 0.813609\varepsilon_1 - 0.045651\varepsilon_2, \\ n_{11} &= -1.052071, & n_{02} &= 1.818182 + 8.978676\varepsilon_1 + 0.311538\varepsilon_2. \end{aligned}$$

Letting $u_2 = u_1, v_2 = v_1(1 - n_{02}u_1)$, we get system (A.3) as follows

$$\begin{cases} \dot{u}_2 = v_2, \\ \dot{v}_2 = \theta_{00} + \theta_{10}u_2 + \theta_{01}v_2 + \theta_{20}u_2^2 + \theta_{11}u_2v_2 + O(|u_2, v_2, \varepsilon_1, \varepsilon_2|^3), \end{cases} \quad (\text{A.3})$$

where

$$\begin{aligned} \theta_{00} &= 0.003864\varepsilon_2, & \theta_{10} &= -0.007026\varepsilon_2, & \theta_{01} &= -\varepsilon_1 - 0.069395\varepsilon_2, \\ \theta_{20} &= -0.139409 - 0.813609\varepsilon_1 - 0.058426\varepsilon_2, & \theta_{11} &= -1.052071 + 1.818182\varepsilon_1 + 0.126173\varepsilon_2. \end{aligned}$$

For small ε_i ($i = 1, 2$), $\theta_{20} < 0$, by the following change of variables

$$u_3 = u_2, \quad v_3 = \frac{v_2}{\sqrt{-\theta_{20}}}, \quad t \rightarrow \sqrt{-\theta_{20}}t,$$

system (A.3) becomes

$$\begin{cases} \dot{u}_3 = v_3, \\ \dot{v}_3 = s_{00} + s_{10}u_3 + s_{01}v_3 - u_3^2 + s_{11}u_3v_3 + O(|u_3, v_3, \varepsilon_1, \varepsilon_2|^3), \end{cases} \quad (\text{A.4})$$

where

$$\begin{aligned} s_{00} &= 0.027720\varepsilon_2, & s_{10} &= -0.050400\varepsilon_2, & s_{01} &= -2.678273\varepsilon_1 - 0.185859\varepsilon_2, \\ s_{11} &= -2.817733 + 13.091929\varepsilon_2 + 0.928379\varepsilon_2. \end{aligned}$$

To eliminate the u_3 term, letting $u_4 = u_3 - \frac{s_{10}}{2}$, $v_4 = v_3$, we get system (A.5) as follows

$$\begin{cases} \dot{u}_4 = v_4, \\ \dot{v}_4 = r_{00} + r_{01}v_4 - u_4^2 + r_{11}u_4v_4 + O(|u_4, v_4, \varepsilon_1, \varepsilon_2|^3), \end{cases} \quad (\text{A.5})$$

where

$$\begin{aligned} r_{00} &= 0.027720\varepsilon_2, & r_{01} &= -2.678273\varepsilon_1 - 0.114852\varepsilon_2, \\ r_{11} &= -2.817733 + 13.091929\varepsilon_1 + 0.928379\varepsilon_2. \end{aligned}$$

Setting $u_5 = -r_{11}^2u_4$, $v_5 = r_{11}^3v_4$, $\tau = -\frac{1}{r_{11}}t$, we obtain the universal unfolding of system (A.6)

$$\begin{cases} \dot{u}_5 = v_5, \\ \dot{v}_5 = \mu_1 + \mu_2v_5 + u_5^2 + u_5v_5 + O(|u_5, v_5, \varepsilon_1, \varepsilon_2|^3), \end{cases} \quad (\text{A.6})$$

where

$$\mu_1 = -1.747416\varepsilon_2, \quad \mu_2 = -7.546659\varepsilon_1 - 0.323622\varepsilon_2. \quad (\text{A.7})$$

- 1) The saddle-node bifurcation curve $\text{SN} = \{(\varepsilon_1, \varepsilon_2) : \mu_1(\varepsilon_1, \varepsilon_2) = 0, \mu_2(\varepsilon_1, \varepsilon_2) \neq 0\}$;
- 2) The Hopf bifurcation curve $\text{H} = \{(\varepsilon_1, \varepsilon_2) : \mu_2(\varepsilon_1, \varepsilon_2) = \pm \sqrt{-\mu_1(\varepsilon_1, \varepsilon_2)}, \mu_1(\varepsilon_1, \varepsilon_2) < 0\}$;
- 3) The homoclinic bifurcation curve $\text{HOM} = \{(\varepsilon_1, \varepsilon_2) : \mu_2(\varepsilon_1, \varepsilon_2) = \pm \sqrt[5]{-\mu_1(\varepsilon_1, \varepsilon_2)}, \mu_1(\varepsilon_1, \varepsilon_2) < 0\}$.

With the specific parameters, we have

1) The saddle-node bifurcation curve, denoted SN, is expressed as

$$\{(\varepsilon_1, \varepsilon_2) : \varepsilon_2 = 0, \varepsilon_1 < 0\};$$

2) The Hopf bifurcation curve, denoted H, is expressed as

$$\{(\varepsilon_1, \varepsilon_2) : -1.74742\varepsilon_2 + 56.9521\varepsilon_1^2 + 37.3603\varepsilon_1\varepsilon_2 + 3.09997\varepsilon_2^2 = 0, \varepsilon_1 < 0\};$$

3) The homoclinic bifurcation curve, denoted HOM, is expressed as

$$\{(\varepsilon_1, \varepsilon_2) : -1.74742\varepsilon_2 + 111.626\varepsilon_1^2 + 42.0495\varepsilon_1\varepsilon_2 + 3.20051\varepsilon_2^2 = 0, \varepsilon_1 < 0\}.$$



AIMS Press

© 2023 the Author(s), licensee AIMS Press. This is an open access article distributed under the terms of the Creative Commons Attribution License (<http://creativecommons.org/licenses/by/4.0>)